Am J Transl Res 2021;13(11):12440-12460
www.ajtr.org /ISSN:1943-8141/AJTR0136070

Original Article

LangChuangHeJi decoction ameliorates lupus via preventing accumulation of CD138+ T cells in MRL/lpr mice

Tianhong Xie[1], Xin Liu[1], Huiqiang Liu[2], Xuyang Han[1], Jingxia Zhao[1], Dongmei Zhou[3], Yan Wang[1], Hongkai Zhang[2], Ping Wang[3], Ping Li[1]

[1]Beijing Hospital of Traditional Chinese Medicine, Capital Medical University, Beijing Institute of Traditional Chinese Medicine, Beijing 100010, China; Departments of [2]Pathology, [3]Dermatology, Beijing Hospital of Traditional Chinese Medicine, Capital Medical University, Beijing 100010, China

Received June 6, 2021; Accepted October 8, 2021; Epub November 15, 2021; Published November 30, 2021

Abstract: LangChuangHeJi (LCHJ) decoction has been used as a supplementary therapy to reduce the dose of prednisone and improve the therapeutic effects in systemic lupus erythematosus (SLE) maintenance. We aimed to explore the underlying mechanisms of the therapeutic effects of LCHJ. Spleen and lymph node weight, renal tissue histology, anti-dsDNA and anti-nuclear antibody levels in serum, and urinary protein levels were measured to evaluate the therapeutic effects. We further measured serum levels of multiple cytokines and antibody subsets, and performed flow cytometry analysis to observe effects of LCHJ on the frequency and activation of T cells and T cell subsets, as well as accumulation of plasma cells in splenocytes of MRL/lpr mice. LCHJ exhibited significant therapeutic effects on MRL/lpr mice. LCHJ significantly controlled the in vivo inflammation and dramatically prevented the accumulation of DN T and plasma cells in MRL/lpr mice. Moreover, LCHJ significantly suppressed the accumulation of CD138+ T cells in MRL/lpr mice, which led to the decreased production of the anti-dsDNA antibody in vivo. LCHJ significantly decreased CD4+CD138+ T cells originated from CD4+CD138- T cells, which subsequently prevented the accumulation of CD138+ T cells in MRL/lpr mice. Our results indicated that LCHJ alleviated renal injuries and prevented the enlargement of the spleen and lymph nodes by suppressing DN T cell accumulation, and reduced anti-dsDNA antibody secretion by preventing the accumulation of CD138+ T cells.

Keywords: CD138+ T cells, DN T cells, T cells, inflammation, decoction, systemic lupus erythematosus

Introduction

Systemic lupus erythematosus (SLE) is a chronic and multisystem autoimmune disease that predominantly affects women, especially between puberty and menopause [1, 2]. It is characterized by the production of autoantibodies [3, 4], including anti-nuclear antibody (ANA) and double-stranded DNA (dsDNA) antibody. Epidemiological research indicates that SLE has a variable incidence rate and prevalence in different regions and environments worldwide [5-7]. Moreover, mortality in patients with SLE remains high with significant geographic variations, despite advances in treatment of SLE in recent years [1, 8, 9].

Glucocorticoids are still the preferred first-line treatment, playing an irreplaceable role in the treatment of SLE, despite the development of therapeutic drugs [10-13]. Oral administration of prednisone was conventionally applied for maintenance treatment for patients who were in remission and proven effective [10-13]. Although SLE can induce severe and irreversible damage, chronic administration of prednisone also contribute to damage or has substantial side effects in patients with SLE [13-16]. Therefore, a treatment option with fewer side effects is required to substitute glucocorticoids or reduce their dose, especially for patients who are administered with prednisone for SLE management.

LangChuangHeJi (LCHJ), a traditional medicine decoction, was clinically applied for the treatment of patients with SLE in remission. LCHJ does not replace prednisone but instead, was

Table 1. Composition of the LangChuangHeJi decoction (LCHJ)

Chinese name	Latin name	Scientific name	Weight (g)	Parts used	Voucher number
Tai Zi Shen	Radix Pseudostellariae	*Pseudostellaria heterophylla (Miq.) Pax*	15 (3/53)	Root Tuber	18122503
Bai Zhu	Atractylodes macrocephala	*Atractylodes macrocephala Koidz*	10 (2/53)	Rhizome	1806005
Huang Qi	Radix Astragali	*Astragalus mongholicus Bunge*	30 (6/53)	Root	19042001
Fu Ling	Poria Cocos	*Poria cocos (Schw.) Wolf*	10 (2/53)	Sclerotium	19051403
Nv Zhen Zi	Fructus Ligustri Lucidi	*Ligustrum lucidum W. T. Aiton*	30 (6/53)	Fruit	19040603
Tu Si Zi	Semen Cuscuta	*Cuscuta chinensis Lam*	15 (3/53)	Seed	19032201
Yin Yang Huo	Epimedium	*Epimedium brevicornu Maxim*	10 (2/53)	Leaf	1903018
Che Qian Zi	Semen Plantaginis	*Plantago asiatica L*	15 (3/53)	Seed	19022002
Bai Hua She She Cao	Hedyotis Diffusa	*Scleromitrion diffusum (Willd.) R. J. Wang*	30 (6/53)	Herb	19032602
Dan Shen	Salvia Miltiorrhiza	*Salvia miltiorrhiza Bunge*	15 (3/53)	Rhizome	19032601
Ji Xue Teng	Caulis Spatholobi	*Spatholobus suberectus Dunn*	30 (6/53)	Rattan Stem	19030802
Qin Jiao	Gentiana Macrophylla	*Gentiana macrophylla Pall*	30 (6/53)	Root	18070901
Gui Zhi	Ramulus Cinnamomi	*Cinnamomum cassia (L.) J. Presl*	10 (2/53)	Twig	18122401
Quan Shen	Rhizoma Bistortae	*Bistorta officinalis Delarbre*	15 (3/53)	Rhizome	19030702

usually used as a supplement therapy combined with prednisone to reduce its dose and improve its therapeutic effects on SLE in remission [17]. The advantage of LCHJ application in SLE management is the safety of long-term administration and significant improvement of the symptoms of patients with SLE according to our previous clinical research [17-19]. LCHJ also exhibited significant therapeutic effects on SLE model mice. Previous results indicated that LCHJ dramatically reduced ANA levels in serum, urinary protein levels, IgG and C3 deposition in kidneys, and improved renal injury in BXSB mice [18, 19].

However, the underlying mechanism of LCHJ treatment remains unclear. In the present study, we aimed to investigate further the effect of LCHJ treatment on MRL/lpr mice and explore the advantages and underlying mechanisms of LCHJ and prednisone combined treatment on SLE.

Materials and methods

Animals

Female MRL/MPJ-lpr mice (4 weeks old) were obtained from the Slac Laboratory (ShangHai, China). All animal experiments were approved by the Beijing Institute of Traditional Chinese Medicine (Ethical Approval Number: 20-19050201).

Preparation of LCHJ decoction

LCHJ was composed of 14 crude herbs which were purchased from TCM Pharmacy of Beijing Hospital of Traditional Chinese Medicine, mixed according to the correct mass ratio (**Table 1**), and deposited in Beijing Institute of Traditional Chinese Medicine. Briefly, a total of 265 g of mixed crude drugs was soaked in pure water for 30 min and decocted in 1000 mL pure water for 1 h. The crude decoction was filtered and concentrated to 2.01 g/mL. Then, the concentrated decoction was preserved at 4°C and re-warmed before administration.

Methods and treatments

All MRL/lpr mice were adaptively fed for a week. MRL/lpr mice were randomly grouped according to different treatments as follows: Vehicle (ddH_2O, n=10); LCHJ decoction 0.1 mL/10 g per day (LCHJ, n=10); prednisone 25 μg/10 g per day (PNS, n=10); prednisone 25 μg/10 g per day combined with LLCHJ decoction 0.1 mL/10 g per day (LCHJ+PNS, n=10). LCHJ administration was performed daily from 6 to 16 weeks of age, and prednisone was administered daily from 9 to 16 weeks of age. At the 17th week, all mice were anesthetized for serum collection. Lymph nodes and spleens from MRL/lpr mice were isolated and weighed. Kidneys of MRL/lpr mice were excised for histology analysis.

UPLC-MS/MS analysis of LCHJ decoction

A Waters UPLC-MS/MS spectrometer equipped with a HESI-II probe was employed. Chromatographic conditions were as follows: The positive and negative HESI-II spray voltages were 3.7 and 3.5 KV, respectively, and the capillary temperature was 320°C. Both the sheath gas

and the auxiliary gas were nitrogen at a pressure of 30 and 10 psi, respectively. The heated vaporizer temperature was 300°C. The collision gas was also nitrogen at a pressure of 1.5 mTorr. Mass to charge ratio scanning ranged from 100 to 1500 DA. UPLC system was controlled by the Xcalibur software 2.2 SP 1.48. Data collection and processing was also performed using the same software.

Histology

To evaluate pathological kidney injury in MRL/lpr mice, hematoxylin and eosin, periodic acid-silver metheramine (PASM), periodic acid Schiff (PAS), and Masson trichrome stainings (Masson) were performed, after kidneys were obtained from MRL/lpr mice and embedded in paraffin. Images of renal tissues were captured and analyzed using Image-Pro Plus 6.0 (Media Cybernetics, Rockville, MD, USA). To evaluate IgG deposition in the kidneys, frozen sections were stained with Alexa Fluor 488-conjugated Goat anti-mouse IgG (H+L) after blocking with goat serum. Images of IgG deposits in the kidneys were semi-quantitatively analyzed using Image J (NIH, Bethesda, MD, USA).

Total IgG, anti-dsDNA IgG, and ANA in serum

Serum levels of total IgG, anti-dsDNA IgG, and ANA were determined using ELISA kits (total IgG ELISA kit, Thermo Fisher; anti-dsDNA IgG and ANA ELISA kit, Alpha Diagnostic International, San Antonio, TX, USA), and performed according to the manufacturer's instructions. Optical density was recorded at 450 nm using a microplate reader.

Serum multiple cytokine and antibody subtype levels

Multiple cytokine and antibody subtype levels in the serum were detected using the Luminex assay kits (Thermo Fisher, USA). Luminex assays were performed according to the manufacturer's instructions and analyzed on the Luminex™ platform.

Protein levels in urine

Urinary samples from MRL/lpr mice were collected for 24 h at the 16th week. The concentration of urinary proteins was measured using the Coomassie Brilliant Blue Dye-binding Assay kit and performed according to the manufacturer's instructions (Biokits Tech. Inc, Beijing, China).

Flow cytometry

After the spleen was excised from MRL/lpr mice, single-cell suspension of splenocytes was obtained and filtered using 70 μm cell strainers. Splenocytes were blocked with a CD16/CD32 monoclonal antibody (Thermo Fisher, eBiosience) and Fixation/Permeabilization solution (BD Bioscience) was used before intracellular staining. Cells were stained with fluorescent-conjugated anti-mouse antibodies, and the following antibodies were used for flow cytometry: Anti-CD3 PE-cy7, anti-CD4 FITC, anti-CD8 APC, anti-CD19 APC-cy7, anti-CD138 PE, anti-CD69 PE, and anti-IFN-γ PE-cy7 (Thermo Fisher, eBiosience). All flow cytometry data were analyzed using the Flowjo software (Tree Star) version 10.6 for PC.

Statistical analysis

All data in the present study are presented as the mean ± standard deviation (SD) and analyzed using SPSS software (SPSS, Inc., Chicago, IL, USA). Comparisons were performed for statistical significance using a one-way analysis of variance. Differences with *P* values of less than 0.05 were considered statistically significant.

Results

Identification of chemical components in LCHJ using UPLC-MS/MS analysis

UPLC-MS/MS analysis was employed to identify the chemical components of LCHJ. The total positive (**Figure 1A**) and negative (**Figure 1B**) ion chromatograms showed 34 major components in the LCHJ decoction. The 34 major components in LCHJ including salvianolic acid A, astragaloside I, rutinum, icariine, salidroside, atractylenolide I, gentiopicroside, tanshinone I, and formononetin were shown in **Table 2**.

LCHJ exhibited significant therapeutic effects on MRL/lpr mice

After the administration of LCHJ, spleen and lymph node weight in MRL/lpr mice were significantly decreased, compared with vehicle-treated MRL/lpr mice (**Figure 2B** and **2C**). At the same time, spleen and lymph indices also

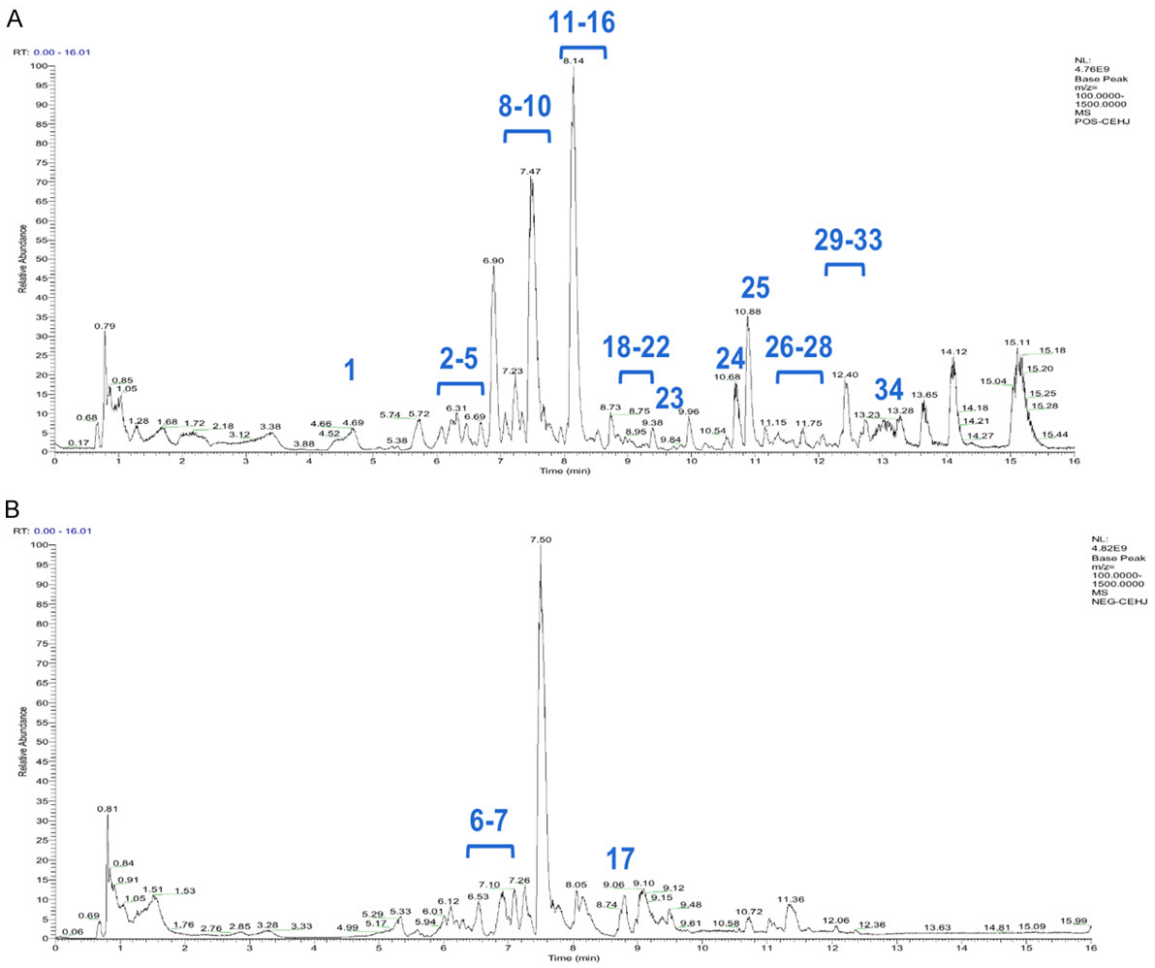

Figure 1. Identification of some components in LCHJ decoction. Base peak ion chromatogram of LCHJ in positive (A) and negative (B) ion modes are shown as indicated.

showed a remarkable decline in MRL/lpr mice after LCHJ treatment (**Figure 2A** and **2C**). Treatment with prednisone alone and combined with LCHJ, also alleviated the enlargement of spleen and lymph node, decreasing spleen and lymph indices (**Figure 2A-C**). Our results indicated that LCHJ had significant effects on preventing the enlargement of spleen and lymph nodes in MRL/lpr mice.

Next, we observed the effect of LCHJ on pathological injury in kidneys and measured renal histopathology and urinary protein levels in MRL/lpr mice. Hyaline deposits, interstitial and perivascular cellular inflammation, glomerular fibrosis, tubular cell necrosis, cellular crescent formation, and glomerulosclerosis were observed in kidneys of MRL/lpr mice (**Figure 2D**), whereas, all these renal injuries were alleviated after LCHJ treatment. IgG immune complex deposition in renal tissues and urinary protein amount were also reduced in MRL/lpr mice 24 h after LCHJ treatment (**Figure 2E** and **2F**). Prednisone alone and combined LCHJ therapy exerted similar therapeutic effects, improving renal histopathology and reducing IgG immune complex deposition in kidneys, as well as reducing protein amounts in urine after 24 h (**Figure 2D-F**).

ANA and anti-dsDNA antibody levels in serum were also measured to evaluate the therapeutic effect of LCHJ on MRL/lpr mice. After 10 weeks of LCHJ treatment, serum ANA and anti-dsDNA antibody levels in MRL/lpr mice were decreased notably (**Figure 2G**), while prednisone alone and LCHJ combined therapy also significantly reduced ANA and anti-dsDNA antibody levels in the serum of MRL/lpr mice (**Figure 2G**). Our results demonstrated that

Table 2. Characterization of chemical components in LCHJ decoction using UPLC-MS/MS analysis

Peak no	Identification	t_R (min)	Ion mode	Measured $[M-H]^-$ (m/z)	Predicted $[M-H]^-$ (m/z)	Δppm	Formula	Drive from
1	Phenylalanine	4.69	ESI+	166.086	166.0862	-1.20	C9H11N02	A, D
2	Tryptophan	6.07	ESI+	205.0968	205.0971	-1.46	C11H12N2O2	A
3	Plantamajoside	6.15	ESI+	641.2071	641.2076	-0.78	C29H36016	H
4	Salvianic acid A	6.29	ESI+	199.0599	199.0601	-1.00	C9H1005	J
5	Salidroside	6.46	ESI+	301.1275	301.1281	-1.99	C14H2007	E
6	Gentiopicroside	6.83	ESI-	355.1039	355.1023	4.51	C16H2009	L
7	Loganic acid	7.23	ESI-	375.1292	375.1285	1.87	C16H24010	L
8	L-Epicatechin	7.33	ESI+	291.0856	291.0863	-2.41	C15H1406	K
9	tyrosine	7.34	ESI+	182.0808	182.0811	-1.65	C9H11N03	A
10	Ferulic acid	7.47	ESI+	195.0647	195.0651	-2.05	C10H1004	I, L
11	Hyperoside	8.01	ESI+	465.1022	465.1027	-1.08	C21H20012	F
12	Astragalin	8.2	ESI+	449.1069	449.1078	-2.00	C21H20011	F
13	Calycosin-7-glucoside	8.26	ESI+	447.1275	447.1285	-2.23	C22H22010	C
14	Rutinum	8.35	ESI+	611.1595	611.1606	-1.80	C27H30016	E
15	Isoacteoside	8.36	ESI+	625.2121	625.2126	-0.80	C29H36015	H
16	Specnuezhenide	8.76	ESI+	685.2355	685.2338	2.48	C31H42017	E
17	Acteoside	8.77	ESI-	625.2122	625.2126	-0.64	C29H36015	H
18	Isoquercitrin	8.78	ESI+	465.1017	465.1027	-2.15	C21H20012	F
19	Quercetin	8.79	ESI+	303.0494	303.0505	-3.63	C15H1007	F, N
20	Quercitrin	9.28	ESI+	449.1069	449.1078	-2.00	C21H20011	F
21	Kaempferol	9.28	ESI+	287.0544	287.0555	-3.83	C15H1006	F
22	Isorhamnetin	9.33	ESI+	317.0651	317.0655	-1.26	C16H1207	F
23	Daidzein	9.73	ESI+	255.0645	255.0651	-2.35	C15H1004	K
24	Icariine	10.68	ESI+	677.2419	677.2439	-2.95	C33H40015	G
25	Formononetin	10.97	ESI+	269.08	269.0808	-2.97	C16H1204	K
26	Atractylenolide III	11.63	ESI+	249.1479	249.1485	-2.41	C15H2003	B
27	Atractylenolide I	11.64	ESI+	231.1374	231.138	-2.60	C15H1802	B
28	Costunolide	11.96	ESI+	233.1532	233.1536	-1.72	C15H2002	B
29	Astragaloside A	12.18	ESI+	785.4677	785.4681	-0.51	C41H68014	C
30	Tanshinone I	12.35	ESI+	277.0855	277.0859	-1.44	C18H1203	J
31	Cryptotanshinone	12.4	ESI+	297.1478	297.1485	-2.36	C19H2003	J
32	Astragaloside I	12.44	ESI+	869.4869	869.4893	-2.76	C45H72016	C
33	Tanshinone II A	12.71	ESI+	295.1323	295.1329	-2.03	C19H1803	J
34	Pachymic acid	13	ESI+	529.388	529.3887	-1.32	C33H5205	D

A: Pseudostellaria heterophylla (Miq.) Pax; B: Atractylodes macrocephala Koidz; C: Astragalus mongholicus Bunge; D: Poria cocos (Schw.) Wolf; E: Ligustrum lucidum W. T. Aiton; F: Cuscuta chinensis Lam; G: Epimedium brevicornu Maxim; H: Plantago asiatica L; I: Scleromitrion diffusum (Willd.) R. J. Wang; J: Salvia miltiorrhiza Bunge; K: Spatholobus suberectus Dunn; L: Gentiana macrophylla Pall; M: Cinnamomum cassia (L.) J. Presl; N: Bistorta officinalis Delarbre.

LCHJ had significant therapeutic effects on MRL/lpr mice.

Oral administration of LCHJ significantly prevented the accumulation of DN T cells in MRL/lpr mice

First, we investigated the effects of LCHJ on the frequency of CD3+ T and CD19+ B cells in MRL/lpr mice. Treatment with LCHJ prevented the increase in the frequency of CD3+ T cells and elevated the percentage of CD19+ B cells in splenocytes of MRL/lpr mice (**Figure 3A** and **3C**). LCHJ combined therapy with prednisone also had similar effects on CD3+ T and CD19+ B cells, while prednisone alone did not (**Figure 3A** and **3C**).

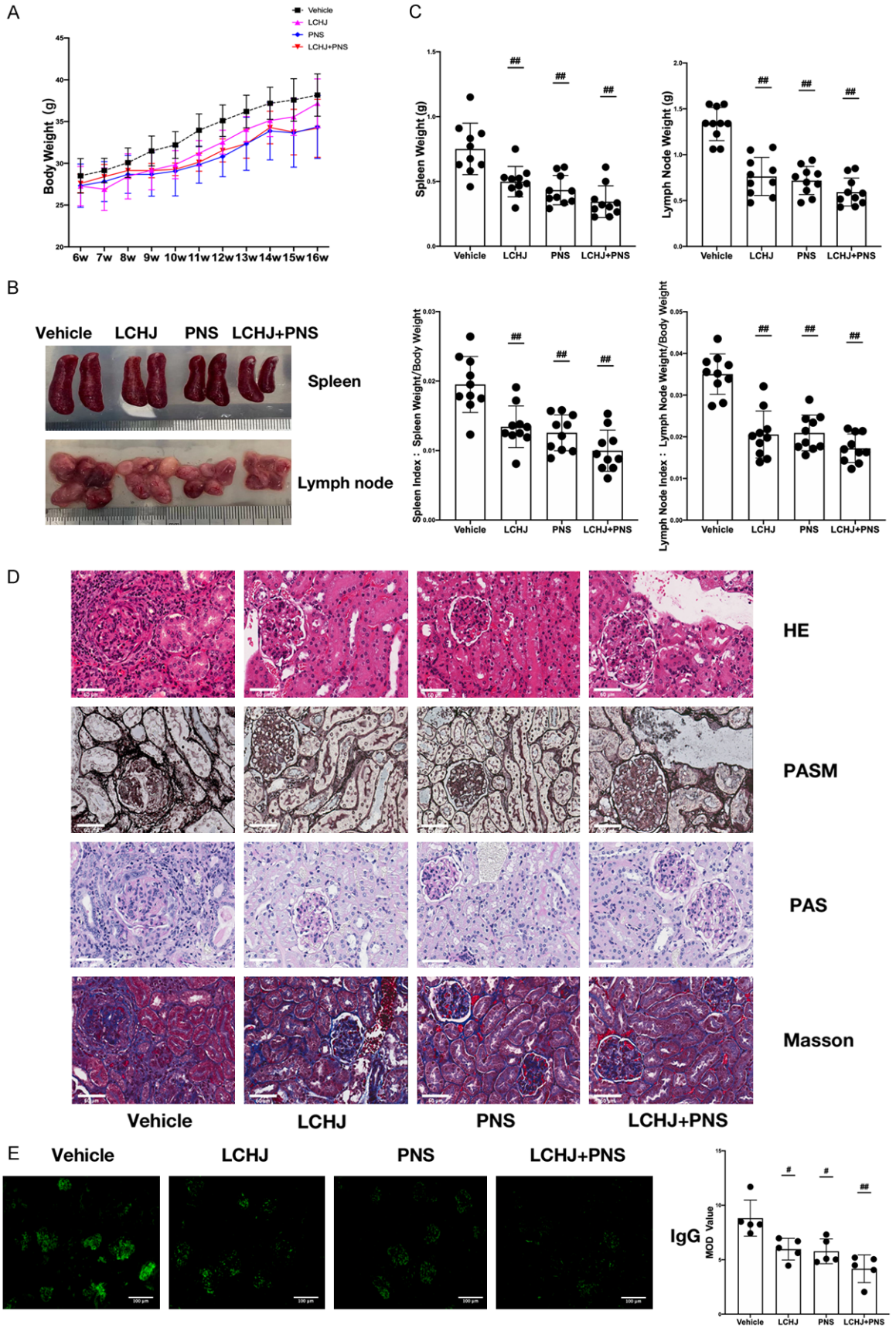
A
Vehicle
LCHJ
PNS
LCHJ+PNS
Body Weight (g)
6w 7w 8w 9w 10w 11w 12w 13w 14w 15w 16w
B
Vehicle LCHJ PNS LCHJ+PNS
Spleen
Lymph node
C
Spleen Weight (g)
Lymph Node Weight (g)
Spleen Index : Spleen Weight/Body Weight
Lymph Node Index : Lymph Node Weight/Body Weight
##
Vehicle LCHJ PNS LCHJ+PNS
D
HE
PASM
PAS
Masson
Vehicle LCHJ PNS LCHJ+PNS
E
Vehicle LCHJ PNS LCHJ+PNS
IgG
MOD Value
#
##
Vehicle LCHJ PNS LCHJ+PNS

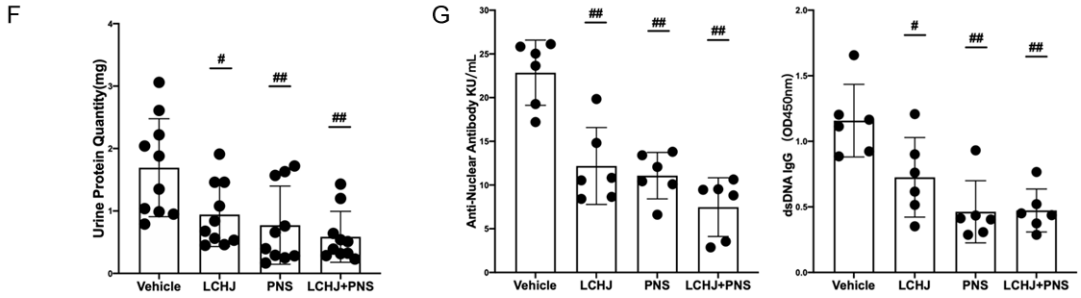

Figure 2. Therapeutic effects of LCHJ on lupus in MRL/lpr mice. A. Body weight of MRL/lpr mice, n=10 per group. B. Image of the spleen (Top panel) and lymph nodes (bottom panel) in MRL/lpr mice. C. Spleen weight, spleen index, lymph node weight, and lymph node index in MRL/lpr mice; n=10 per group. D. Renal tissue pathological sections were stained with HE, PASM, PAS, and Masson, original magnification: 400×, scale bar =60 μm; n=4 per group. E. Representative frozen stained sections with Alexa Flour 488-conjugated goat anti-mouse IgG (H+L) to determine IgG deposits level, original magnification: 200×, scale bar =100 μm; n=5 per group. F. Urinary protein quantity; n=10 per group. G. ANA and anti-dsDNA antibody levels in the serum of MRL/lpr mice were measured using ELISA; n=6 per group. Data are presented as the mean ± SD; $^{\#}P<0.05$, $^{\#\#}P<0.01$ by one-way analysis of variance, versus vehicle-treated mice.

Next, we observed the change in T cell subset frequency in splenocytes of MRL/lpr mice. Our results showed that more than 50% of accumulated CD3+ T cells in vehicle-treated MRL/lpr mice were DN T cells. Besides, LCHJ exhibited significant effects on preventing the accumulation of DN T cells and the percentage of DN T cells among CD3+ T cells was significantly reduced in MRL/lpr mice treated with LCHJ (**Figure 3B**). However, prednisone alone did not show significant effects on reducing DN T cell frequency among CD3+ T cells (**Figure 3B**). LCHJ combined treatment with prednisone also prevented the accumulation of DN T cells in MRL/lpr mice and reduced the DN T cells proportion among CD3+ T cells (**Figure 3B**), while LCHJ, prednisone, and combined treatment did not exhibit obvious effects on the frequency of CD4+ T and CD8+ T cells in MRL/lpr mice (**Figure 3D** and **3E**). Our results indicated that LCHJ significantly prevented the accumulation of DN T cells in MRL/lpr mice.

LCHJ and prednisone combined treatment prevented activation and proliferation of T cells and T cell subsets in MRL/lpr mice

We further elucidate the effect of LCHJ treatment on the activation and proliferation of T cells. We stimulated splenocytes obtained from MRL/lpr mice using CpGC with PMA and Ionomycin in vitro for 5 h and measured CD69 expression in T cells and T cell subsets. CD3+ T cells from MRL/lpr mice either after LCHJ or prednisone treatment did not show remarkably decreased CD69 expression in CD3+ T cells after stimulation of splenocytes in vitro (**Figure 4A**). Furthermore, combined LCHJ and prednisone therapy exhibited a significant suppression on CD3+ T cell activation in response to stimulation (**Figure 4A**). We then used CpGC to stimulate splenocytes for 24 h in vitro and observed a change in CD3+ T cell frequency in MRL/lpr mice. Our results showed that only combined LCHJ and prednisone treatment significantly reduced the frequency of CD3+ T cells after CpGC stimulation of splenocytes (**Figure 4B**).

DN T cell frequency among CD3+ T cells was also decreased in MRL/lpr mice treated with LCHJ, prednisone, and their combination after 24 h stimulation of splenocytes in vitro (**Figure 4C**). In contrast, combined treatment with LCHJ and prednisone reduced CD69 frequency among DN T cells in MRL/lpr mice, compared with vehicle-treated MRL/lpr mice (**Figure 4D**). LCHJ, prednisone, and combined therapy significantly decreased CD69 expression in CD8+ T cells, although the CD8+ T cell frequency did not significantly change after 24 h of CpGC stimulation (**Figure 4F**). Additionally, only combined therapy with LCHJ and prednisone exhibited significant effects on reducing the CD69+ cell frequency among CD4+ T cells in MRL/lpr mice (**Figure 4E**). Our results indicated that LCHJ prevented activation and proliferation of CD3+ T cells and T cell subsets in response to stimulation. Importantly, LCHJ combined with prednisone exhibited more significant suppres-

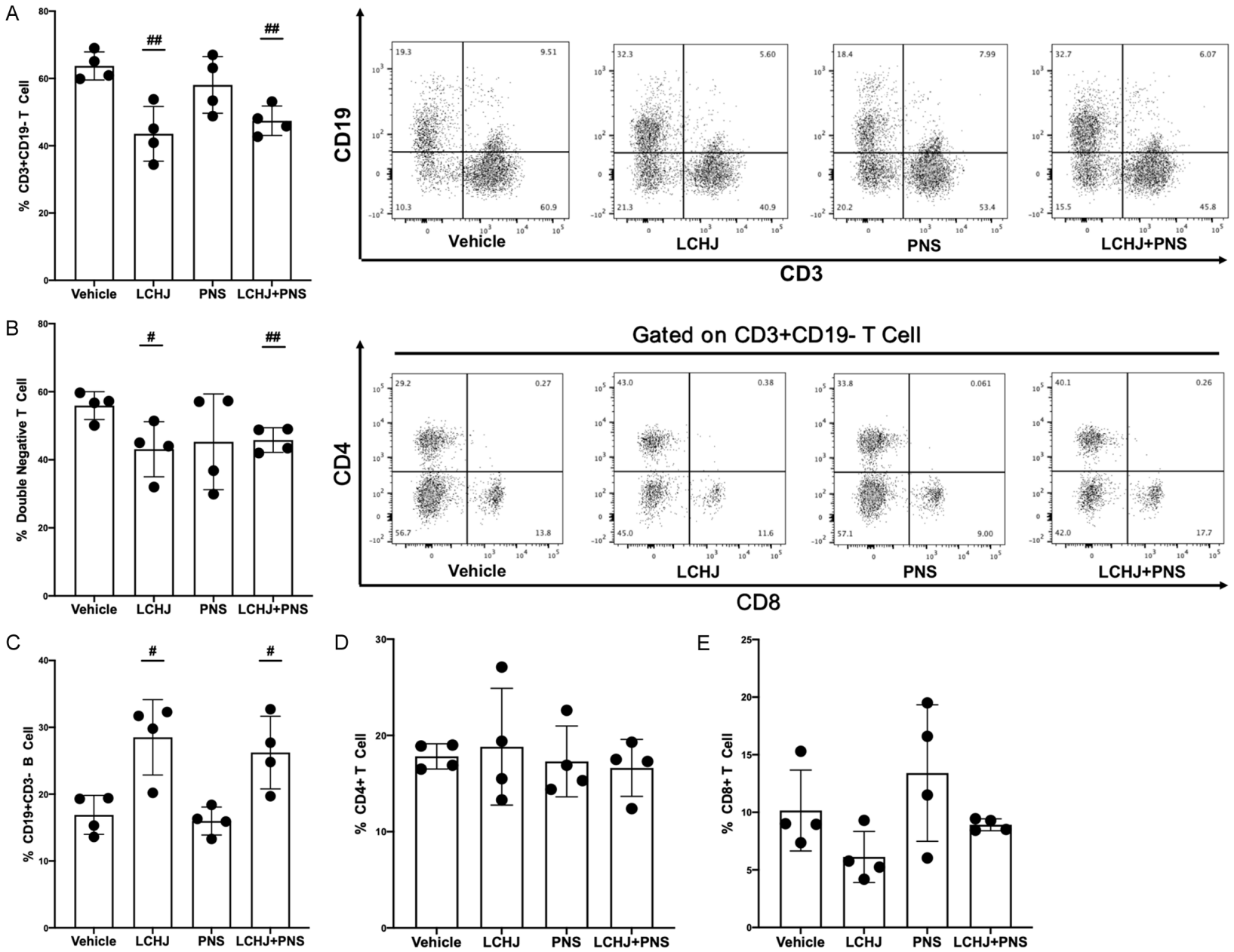
A
% CD3+CD19- T Cell
Vehicle
LCHJ
PNS
LCHJ+PNS
CD19
CD3
19.3
9.51
10.3
60.9
32.3
5.60
21.3
40.9
18.4
7.99
20.2
53.4
32.7
6.07
15.5
45.8
B
% Double Negative T Cell
Gated on CD3+CD19- T Cell
CD4
CD8
29.2
0.27
56.7
13.8
43.0
0.38
45.0
11.6
33.8
0.061
57.1
9.00
40.1
0.26
42.0
17.7
C
% CD19+CD3- B Cell
D
% CD4+ T Cell
E
% CD8+ T Cell

Figure 3. Effects of LCHJ on CD3+ T cells and DN T cells in MRL/lpr mice. A. Flow cytometry of CD3+CD19- T cells in splenocytes in MRL/lpr mice, and scatter plots with bars showing the frequency of CD3+CD19- T cells in splenocytes; n=4 per group. B. Flow cytometry of DN T cells among CD3+ T cells, and scatter plots with bars showing the frequency of DN T cells among CD3+ T cells; n=4 per group. C. Scatter plots with bars showing the frequency of CD19+CD3- B cells in splenocytes in MRL/lpr mice; n=4 per group. D. Scatter plots with bars showing the frequency of CD4+ T cells in splenocytes in MRL/lpr mice; n=4 per group. E. Scatter plots with bars showing the frequency of CD8+ T cells in splenocytes in MRL/lpr mice; n=4 per group. Data are presented as the mean ± SD; $^{\#}P<0.05$, $^{\#\#}P<0.01$, by one-way analysis of variance, versus vehicle-treated mice.

sive effects on T cells and T cell subsets, especially CD4+ T cells and DN T cells, in MRL/lpr mice in response to stimulation.

LCHJ significantly suppressed in vivo inflammation and decreased Th1 frequency in CD4+ T cells in MRL/lpr mice

We explored the effects of LCHJ on inflammation in MRL/lpr mice in vivo. We observed that serum levels of IFN-γ, TNF, and IL-6 were significantly decreased in MRL/lpr mice after treatment with LCHJ, prednisone, and their combination (**Figure 5A**).

Consistent with our results for the serum of MRL/lpr mice, IFN-γ production in CD4+ T cells in LCHJ-treated MRL/lpr mice was significantly reduced both after 5 and 48 h of splenocyte stimulation with anti-CD3 and CpGC in vitro (**Figure 5B** and **5C**). Prednisone alone and combined therapy also significantly reduced IFN-γ expression in CD4+ T cells in MRL/lpr mice (**Figure 5B** and **5C**). Our results indicated that LCHJ suppressed the production of IFN-γ, TNF, and IL-6 in serum and significantly reduced Th1 frequency in CD4+ T cells in MRL/lpr mice.

LCHJ reduced in vivo multiple antibody subset production in serum and prevented the accumulation of plasma cells in MRL/lpr mice

We observed the production of multiple antibody subsets in MRL/lpr mice and explored whether LCHJ affected the secretion of multiple antibody subsets in the serum of MRL/lpr mice. Compared with vehicle-treated mice, total serum IgG and IgG1 levels in LCHJ-treated MRL/lpr mice were significantly reduced (**Figure 6A**). Prednisone-treated MRL/lpr mice exhibited a significant decrease in serum levels of total IgG, IgG1, and IgG2b (**Figure 6A**). Different to total IgG, IgG1, and IgG2b, serum IgG3 levels in MRL/lpr mice was also significantly decreased after combined LCHJ and prednisone treatment (**Figure 6A**).

Next, we investigated whether LCHJ affected plasma cells in MRL/lpr mice. We observed that the percentage of CD138+ cells was significantly decreased in splenocytes in LCHJ-treated MRL/lpr mice both with and without of splenocyte stimulation in vitro with CpGC for 24 h, compared with vehicle-treated MRL/lpr mice (**Figure 6B** and **6C**). Other treatments also had similar effects on CD138+ plasma cell frequency in MRL/lpr mice (**Figure 6B** and **6C**). Our results indicated that LCHJ suppressed the accumulation of plasma cells and reduced the production of in vivo multiple antibody subsets in MRL/lpr mice.

LCHJ reduced the accumulation of CD138+ T cells in MRL/lpr mice

We believed that plasma cells originated from B cells. However, CD3+ plasma cells, i.e. CD138+ T cells, were previously found in MRL/lpr mice as reported in some clinical studies about plasmablastic B-cell neoplasms in recent years [20, 21]. Moreover, it was reported that CD138+ T cells play a role in the development of MRL/lpr mice and contribute to the production of the anti-dsDNA antibody in vivo and in vitro [22]. We investigated whether LCHJ further exerted effects on CD138+ T cells. Without stimulation, there was no obvious difference in CD138+CD3- cell frequency in the splenocytes of LCHJ-treated MRL/lpr mice, compared with that in those of vehicle-treated MRL/lpr mice (**Figure 6D**). However, the percentage of CD138+CD3+ cells in splenocytes in LCHJ-treated MRL/lpr mice was significantly decreased (**Figure 6D**). After 24 h the frequency of CpGC-stimulated splenocytes, both CD138+ CD3+ cells and CD138+CD3- cells, in LCHJ-treated MRL/lpr mice was significantly decreased, compared with that of vehicle-treated mice (**Figure 6E**). Other treatments also exhibited similar therapeutic, including LCHJ, prednisone, and combined therapy (**Figure 6E**).

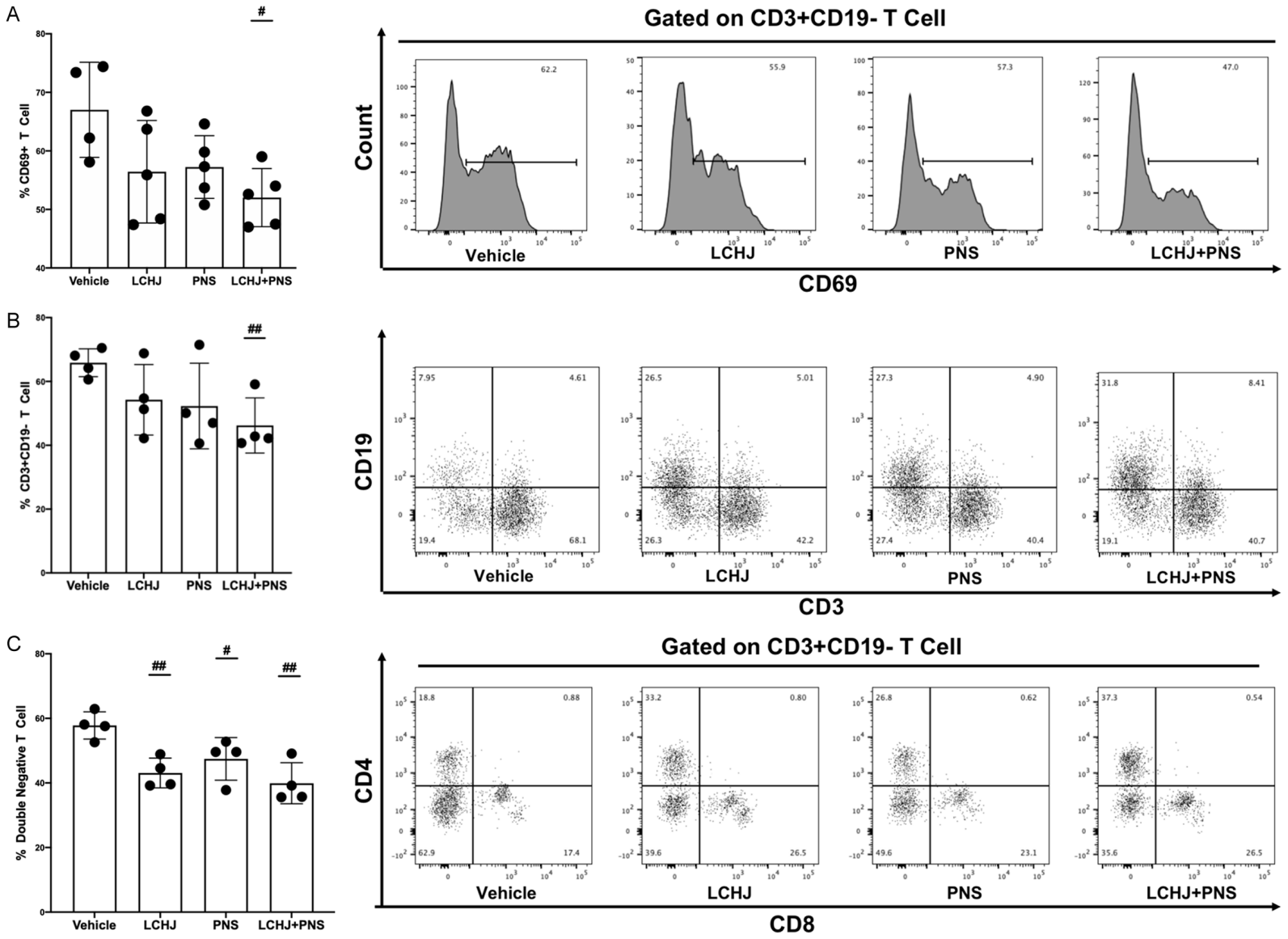
A
% CD69+ T Cell
Vehicle
LCHJ
PNS
LCHJ+PNS
#
Gated on CD3+CD19- T Cell
Count
62.2
55.9
57.3
47.0
CD69
B
% CD3+CD19- T Cell
##
CD19
7.95
4.61
19.4
68.1
26.5
5.01
26.3
42.2
27.3
4.90
27.4
40.4
31.8
8.41
19.1
40.7
CD3
C
% Double Negative T Cell
##
#
##
Gated on CD3+CD19- T Cell
CD4
18.8
0.88
62.9
17.4
33.2
0.80
39.6
26.5
26.8
0.62
49.6
23.1
37.3
0.54
35.6
26.5
CD8

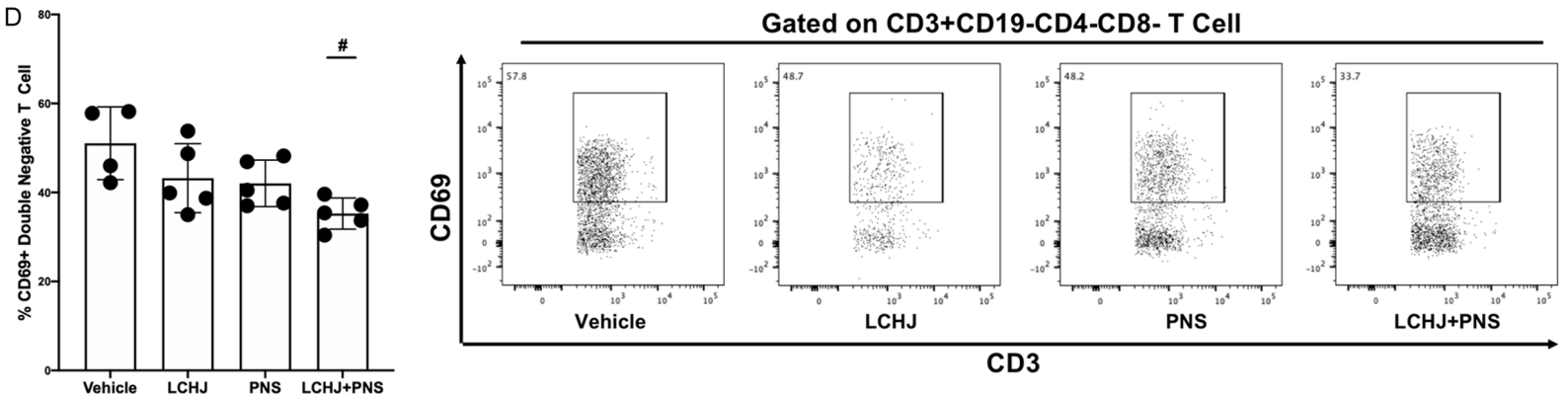
D
% CD69+ Double Negative T Cell
Vehicle
LCHJ
PNS
LCHJ+PNS
#
Gated on CD3+CD19-CD4-CD8- T Cell
CD69
CD3
57.8
48.7
48.2
33.7

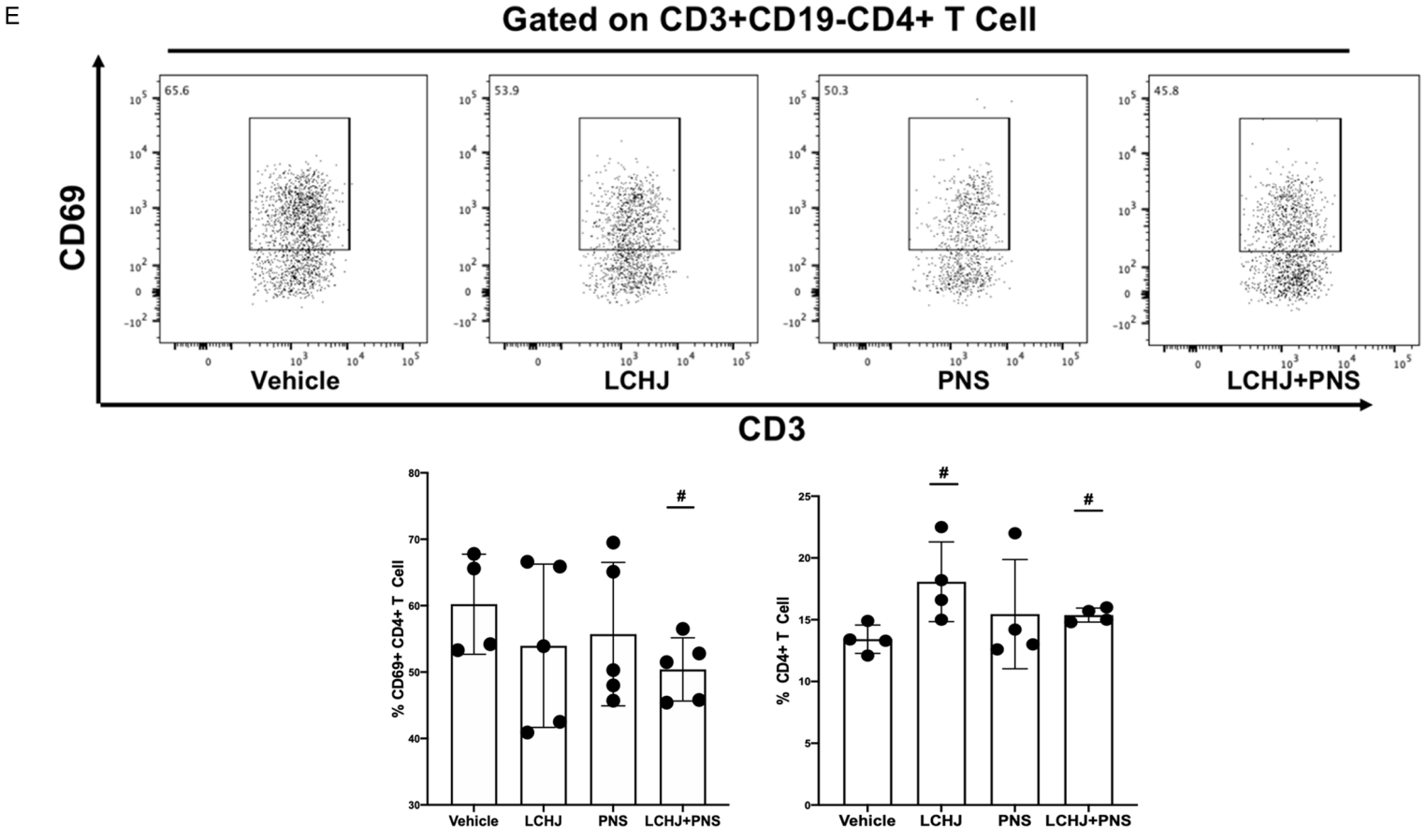
E
Gated on CD3+CD19-CD4+ T Cell
CD69
CD3
65.6
53.9
50.3
45.8
% CD69+ CD4+ T Cell
% CD4+ T Cell
Vehicle
LCHJ
PNS
LCHJ+PNS
#

F

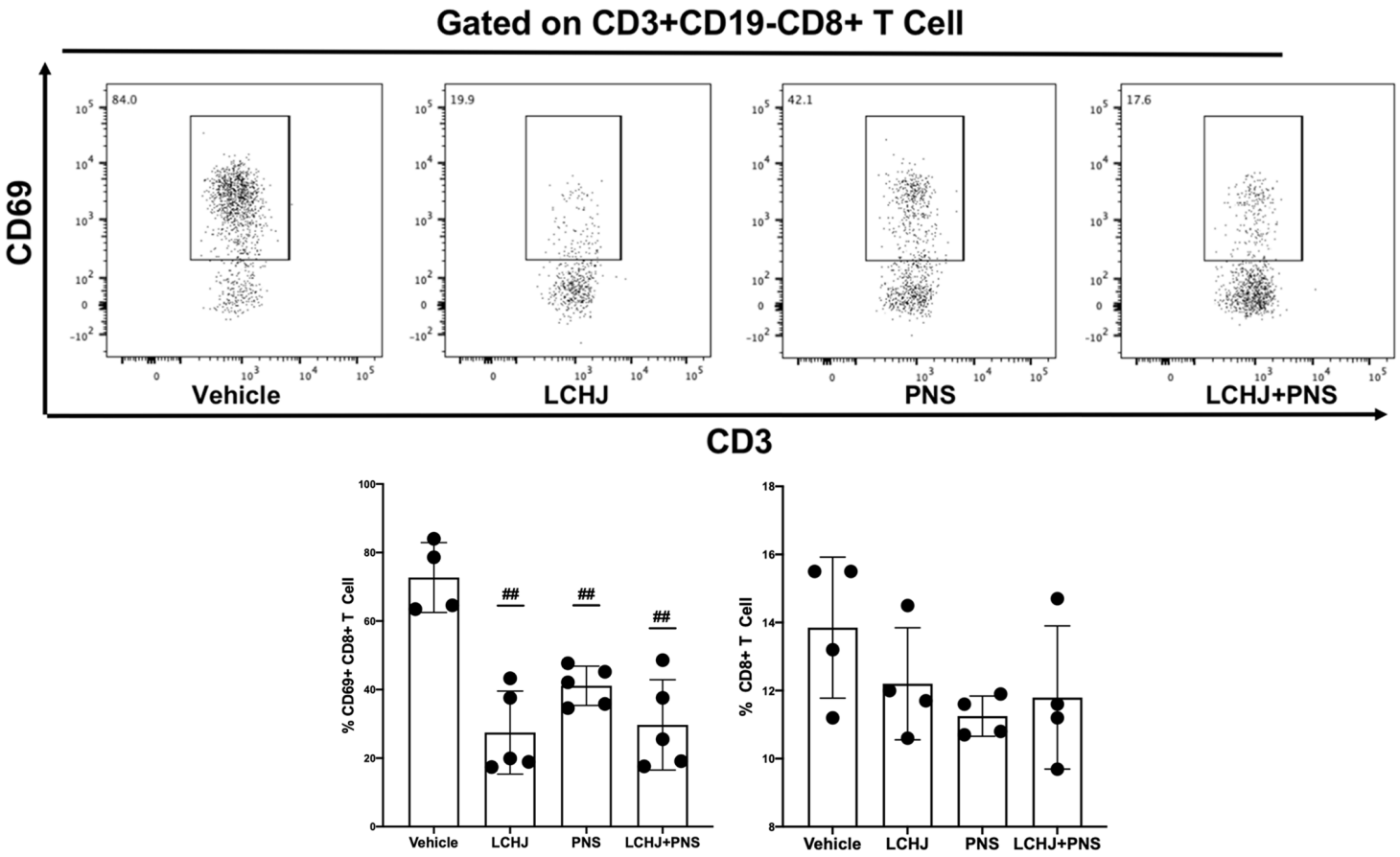

Figure 4. Effects of LCHJ on CD3+ T cells and DN T cells in CpGC stimulation. A. Flow cytometry of CD69 expression in CD3+ T cells in in vitro CpGC-, PMA-, and Ionomycin-stimulated splenocytes of MRL/lpr mice for 5 h and scatter plots with bars showing the frequency of CD69 expressing CD3+ T cells; n=4, 5, 5, 5 per group, respectively. B. Flow cytometry for CD3+CD19- T cells in CpGC-stimulated splenocytes in vitro for 24 h and scatter plots with bars showing the frequency of CD3+CD19- T cells in splenocytes; n=4 per group. C. Flow cytometry of DN T cells among CD3+ T cells in CpGC-stimulated splenocytes in vitro for 24 h and scatter plots with bars showing the frequency of DN T cells among CD3+ T cells; n=4 per group. D. Flow cytometry of CD69+ expression in DN T cells in CpGC-, PMA-, and Ionomycin-stimulated splenocytes of MRL/lpr mice for 5 h and scatter plots with bars showing CD69 expression in DN T cells in MRL/lpr mice; n=4, 5, 5, 5 per group, respectively. E. Flow cytometry of CD69 expression in CD4+ T cells in CpGC-, PMA-, and Ionomycin-stimulated splenocytes in MRL/lpr mice for 5 h; scatter plots with bars showing CD69 expression in CD4+ T cells (n=4, 5, 5, 5 per group, respectively) in CpGC-, PMA-, and Ionomycin-stimulated splenocytes of MRL/lpr mice for 5 h and the frequency of CD4+ T cells in splenocytes (n=4 per group) in MRL/lpr mice after CpGC stimulation for 24 h. F. Flow cytometry of CD69 expression in CD8+ T cells in CpGC-, PMA-, and Ionomycin-stimulated splenocytes of MRL/lpr mice in vitro for 5 h; scatter plots with bars showing CD69 expression in CD8+ T cells (n=4, 5, 5, 5 per group, respectively) in CpGC-, PMA-, and Ionomycin-stimulated splenocytes of MRL/lpr mice in vitro for 5 h and the frequency of CD8+ T cells (n=4 per group) in splenocytes in MRL/lpr mice upon CpGC stimulation in vitro for 24 h. Data are presented as the mean ± SD; $^{\#}P<0.05$, $^{\#\#}P<0.01$, by one-way analysis of variance, versus vehicle-treated mice.

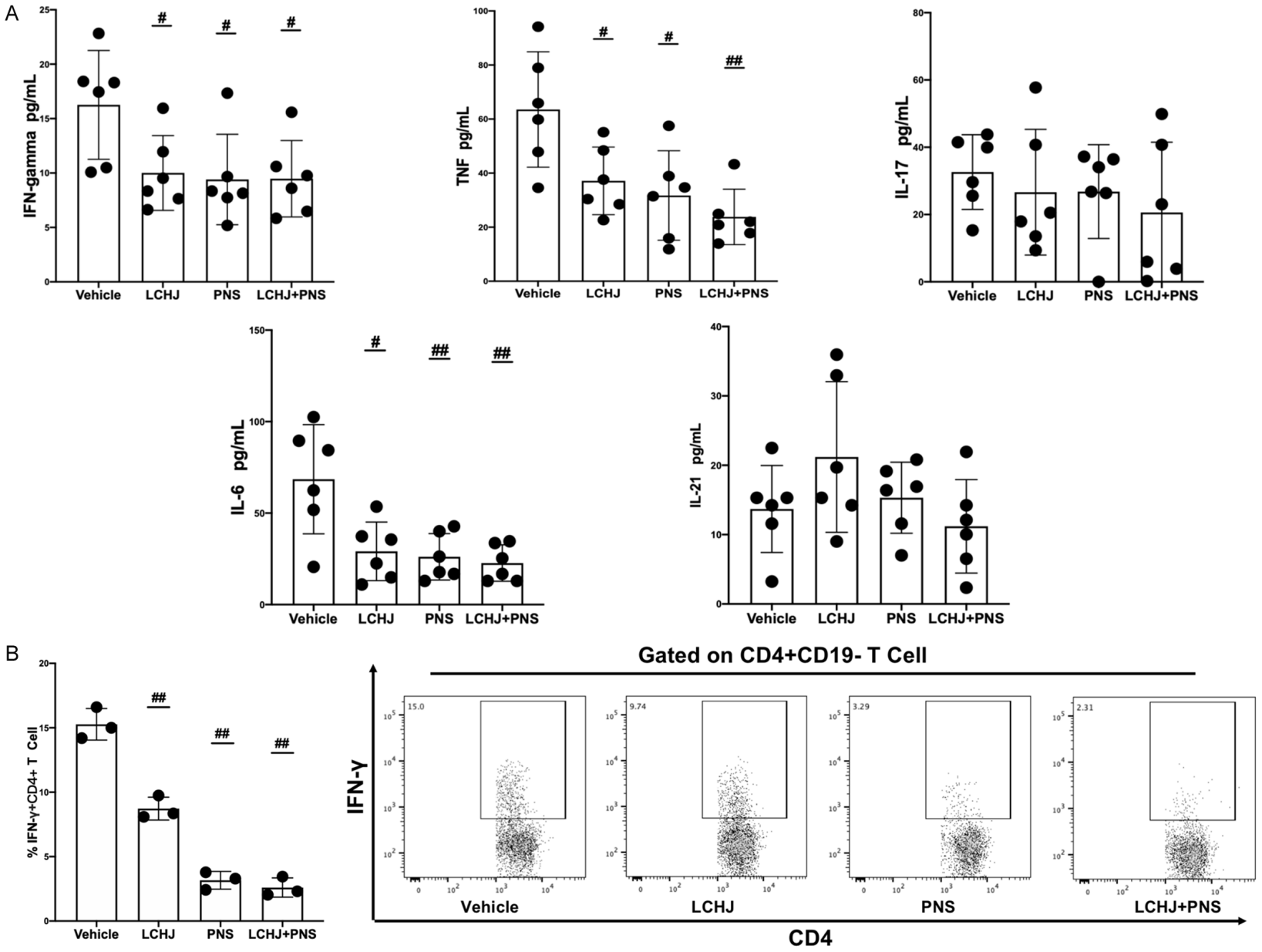
A
IFN-gamma pg/mL
TNF pg/mL
IL-17 pg/mL
IL-6 pg/mL
IL-21 pg/mL
Vehicle
LCHJ
PNS
LCHJ+PNS
B
% IFN-γ+CD4+ T Cell
Gated on CD4+CD19- T Cell
IFN-γ
CD4
15.0
9.74
3.29
2.31

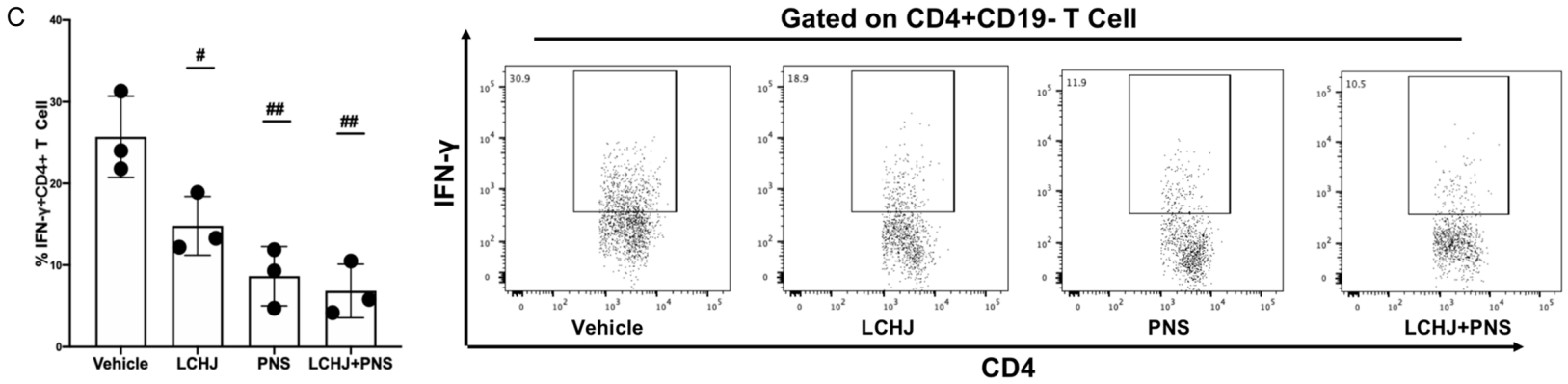

Figure 5. Effects of LCHJ on in vivo inflammation and Th1 cells in MRL/lpr mice. A. Scatter plots with bars showing serum levels of multiple cytokines in MRL/lpr mice measured using Luminex; n=6 per group. B. Flow cytometry of IFN-γ expression in CD4+ T cells in CpGC- and anti-CD3 antibody-stimulated splenocytes of MRL/lpr mice (in vitro for 5 h) and scatter plots with bars showing the frequency of IFN-γ-expressing CD4+ T cells; n=3 per group. C. Flow cytometry of IFN-γ expression in CD4+ T cells in CpGC- and anti-CD3 antibody-stimulated splenocytes of MRL/lpr mice (in vitro for 48 h) and scatter plots with bars showing IFN-γ expression in CD4+ T cells; n=3 per group. Data are presented as the mean ± SD; $^{\#}P<0.05$, $^{\#\#}P<0.01$, by one-way analysis of variance, versus vehicle-treated mice.

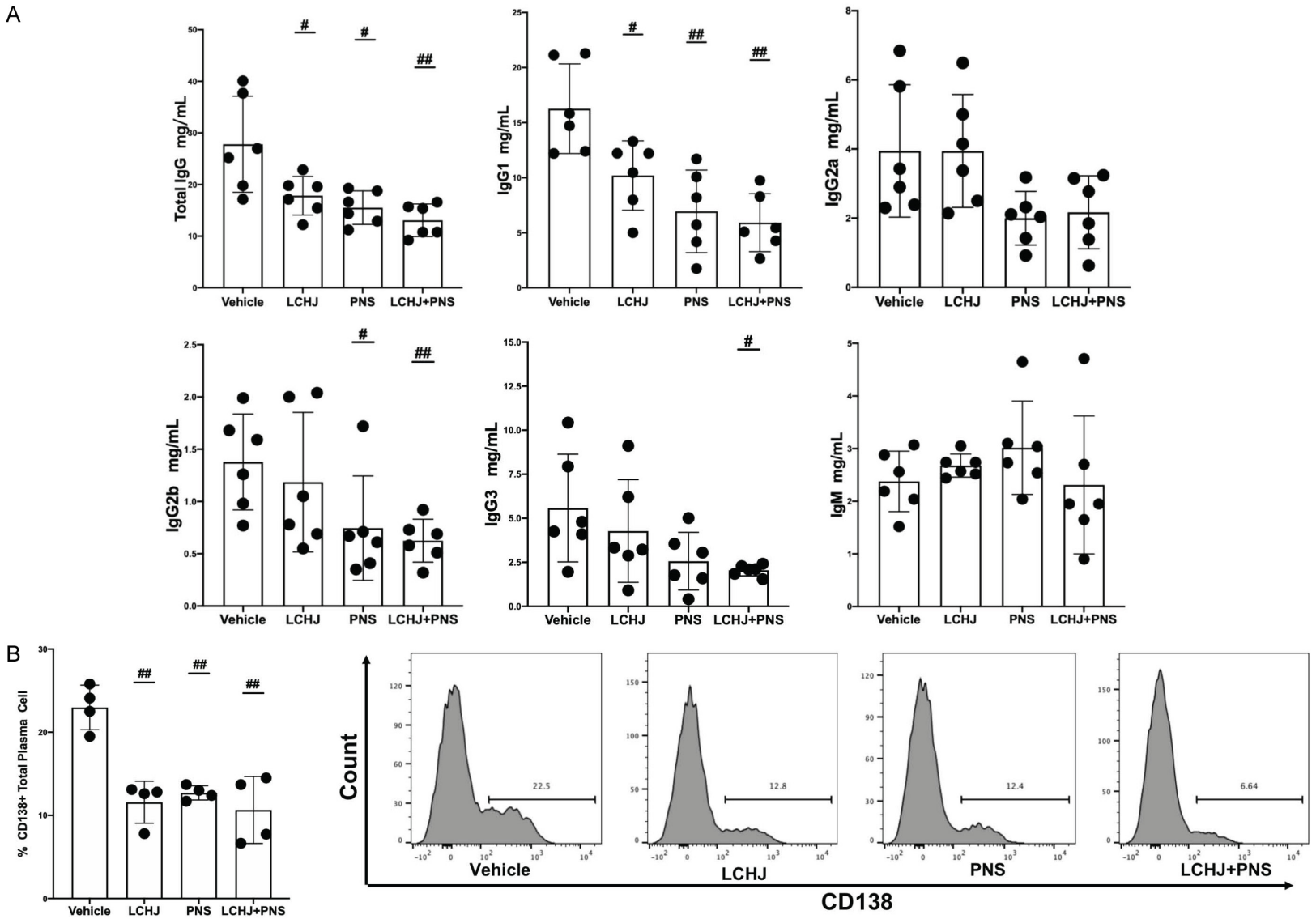
A
Total IgG mg/mL
IgG1 mg/mL
IgG2a mg/mL
IgG2b mg/mL
IgG3 mg/mL
IgM mg/mL
Vehicle
LCHJ
PNS
LCHJ+PNS
#
##
B
% CD138+ Total Plasma Cell
Count
CD138
22.5
12.8
12.4
6.64

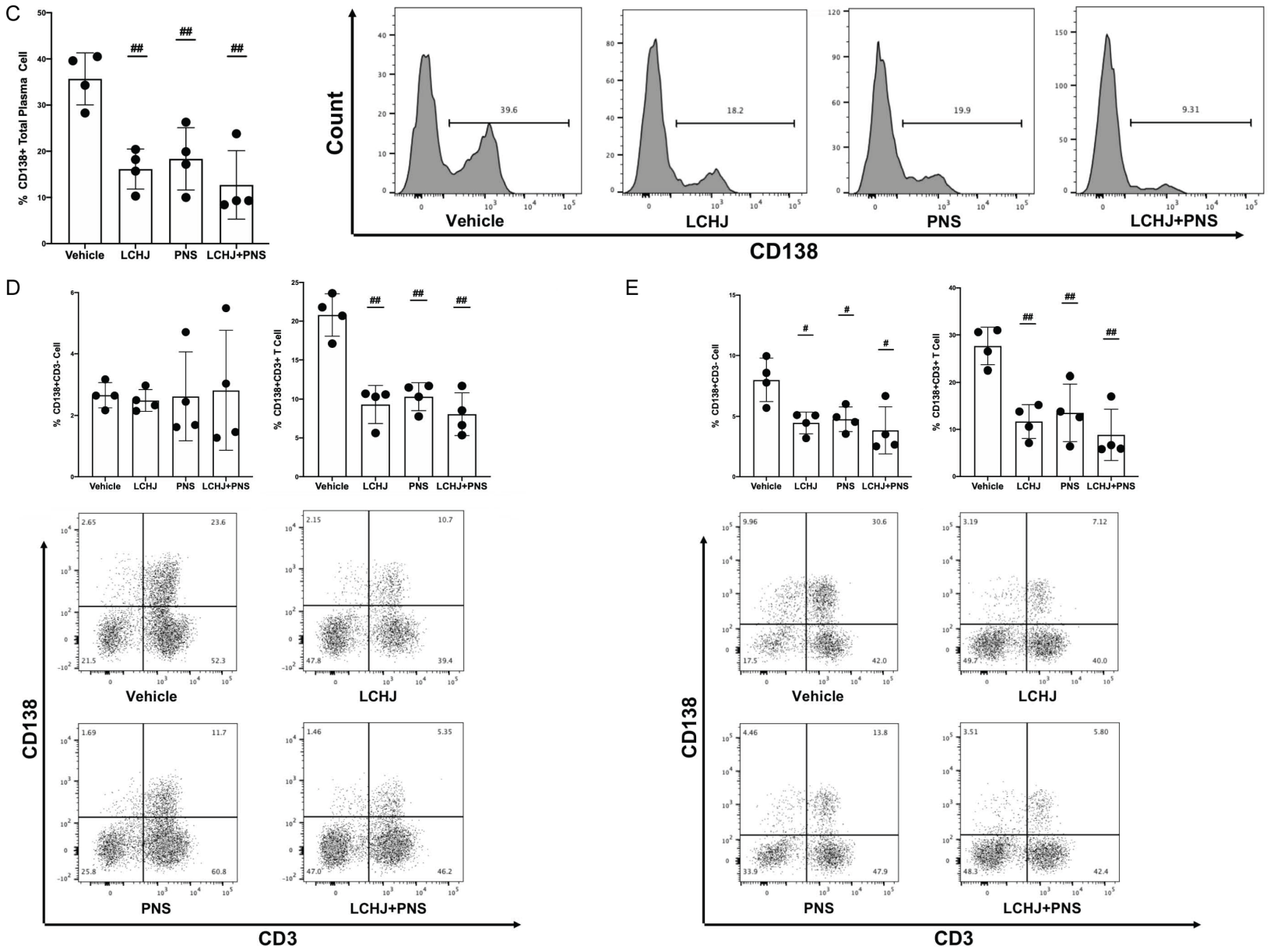
C
% CD138+ Total Plasma Cell
Vehicle
LCHJ
PNS
LCHJ+PNS
Count
39.6
18.2
19.9
9.31
CD138
D
% CD138+CD3- Cell
% CD138+CD3+ T Cell
2.65
23.6
21.5
52.3
2.15
10.7
47.8
39.4
1.69
11.7
25.8
60.8
1.46
5.35
47.0
46.2
CD138
CD3
E
% CD138+CD3- Cell
% CD138+CD3+ T Cell
9.96
30.6
17.5
42.0
3.19
7.12
49.7
40.0
4.46
13.8
33.9
47.9
3.51
5.80
48.3
42.4
CD138
CD3

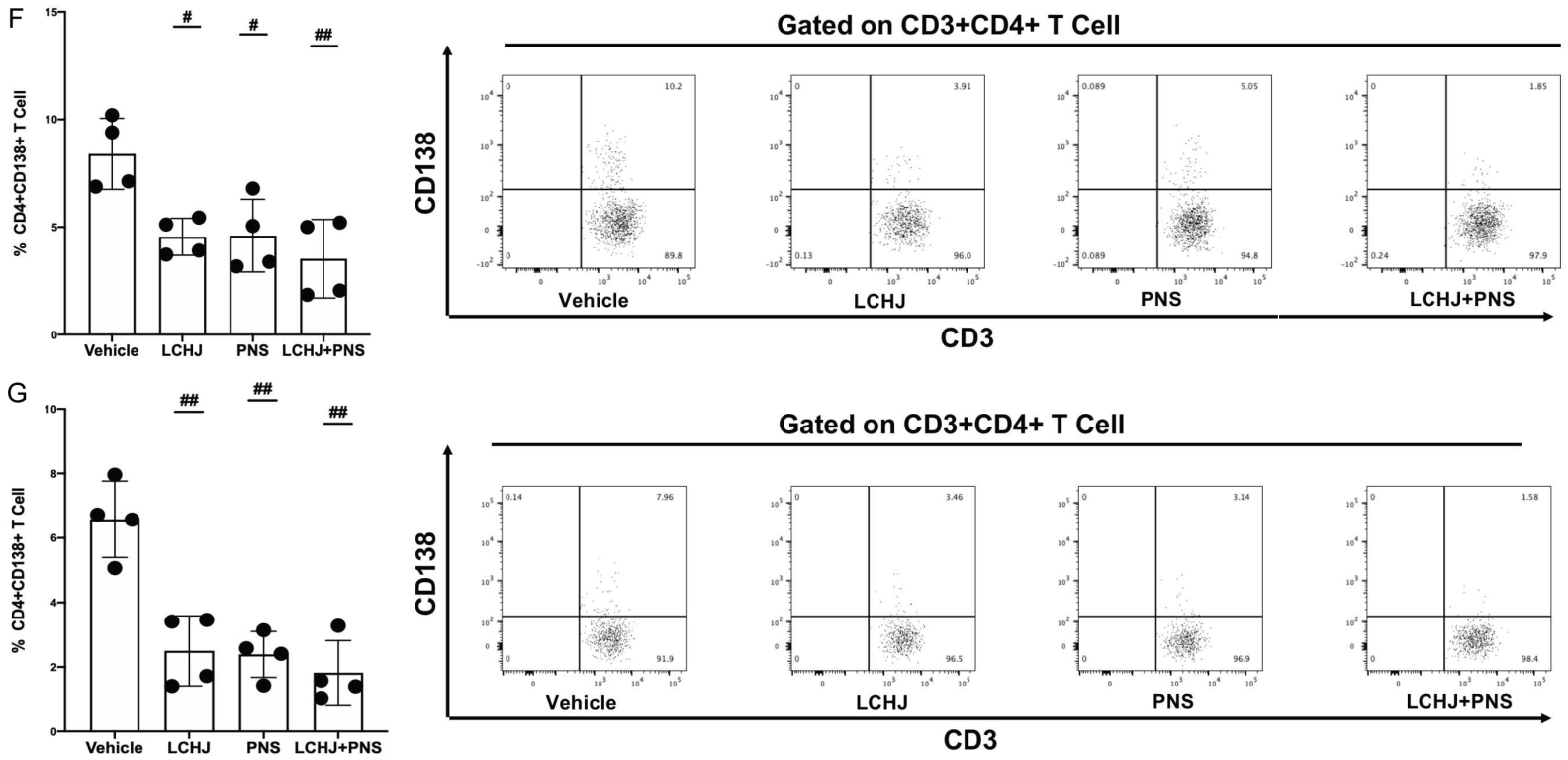

Figure 6. Effects of LCHJ on the production of antibodies in serum and CD138+ plasma cells in MRL/lpr mice. A. Scatter plots with bars showing serum levels of total IgG and multiple antibody subsets in MRL/lpr mice measured using ELISA and Luminex, respectively; n=6 per group. B. Flow cytometry of CD138+ plasma cells in splenocytes of MRL/lpr mice and scatter plots with bars showing the frequency of CD138+ plasma cells in splenocytes; n=4 per group. C. Flow cytometry of CD138+ plasma cells in CpGC-stimulated splenocytes of MRL/lpr mice in vitro for 24 h and scatter plots with bars showing the frequency of CD138+ plasma cells in splenocytes; n=4 per group. D. Flow cytometry of CD138+CD3- and CD138+CD3+ cells in splenocytes of MRL/lpr mice and scatter plots with bars showing the frequency of CD138+CD3- and CD138+CD3+ cells in splenocytes; n=4 per group. E. Flow cytometry of CD138+CD3- and CD138+CD3+ cells in CpGC stimulation of splenocytes in MRL/lpr mice in vitro for 24 hours and scatter plots with bars showing the frequency of CD138+CD3- cells and CD138+CD3+ cells in splenocytes; n=4 per group. F. Flow cytometry of CD4+CD138+ T cells in splenocytes of MRL/lpr mice and scatter plots with bars showing the frequency of CD4+CD138+ T cells in CD4+ T cells; n=4 per group. G. Flow cytometry of CD4+CD138+ T cells in CpGC-stimulated splenocytes of MRL/lpr mice in vitro for 24 h and scatter plots with bars showing the frequency of CD4+CD138+ T cells in CD4+ T cells; n=4 per group. Data are presented as the mean ± SD; $^{\#}P<0.05$, $^{\#\#}P<0.01$, by one-way analysis of variance, versus vehicle-treated mice.

LCHJ reduced the frequency of CD138+ T cells originating from CD4+CD138- T cells in MRL/lpr mice

We further investigated the mechanism of how LCHJ prevented the accumulation of CD138+ T cells and measured the effects of LCHJ on CD138 expression in CD4+ T cells in MRL/lpr mice. Compared with vehicle-treated mice, LCHJ significantly decreased CD138 expression in CD4+ T cells in MRL/lpr mice (**Figure 6F**). After 24 h of splenocyte stimulation with CpGC, CD4+CD138+ T cell frequency among CD4+ T cells was also decreased in LCHJ-treated MRL/lpr mice compared with that in vehicle-treated mice (**Figure 6G**). Prednisone alone and combined treatment also exhibited significant effects on decreasing CD4+CD138+ T cell frequency among CD4+ T cells in MRL/lpr mice both in the absence and presence of CpGC stimulation after 24 h (**Figure 6F** and **6G**). Our results indicated that LCHJ prevented the accumulation of CD138+ T cells by reducing the frequency of CD4+CD138+ T cells originated from CD4+CD138- T cells.

Discussion

In the present study, we have demonstrated that LCHJ had significant therapeutic effects by alleviating the enlargement of the spleen and lymph nodes, improving renal injuries, and decreasing the production of ANA and anti-dsDNA antibodies in MRL/lpr mice. LCHJ had significantly decreased serum levels of cytokines, including IFN-γ, TNF, and IL-6, which causes suppression of the activation and proliferation of CD3+ T cells, reduction of Th1 frequency in CD4+ T cells, and prevention of the accumulation of DN T cells in MRL/lpr mice. LCHJ successfully reduced the production of multiple antibody subsets in the serum and suppressed the accumulation of plasma cells in MRL/lpr mice. LCHJ prevented the accumulation of CD138+ T cells in MRL/lpr mice, which contributed to the decreased production of the anti-dsDNA antibody. Moreover, we have shown that LCHJ significantly decreased CD138 expression in CD4+ T cells, which might constitute the underlying mechanism of how LCHJ prevented the accumulation of CD138+ T cells.

DN T cells are known to play an important role in the development of lupus in MRL/lpr mice [23, 24]. There is evidence that DN T cells participate in the aggravation of certain syndromes and kidney injury in MRL/lpr mice [23]. Our results demonstrated that LCHJ significantly prevented the accumulation of DN T cells in MRL/lpr mice and suppressed the activation of DN T cells. Whether the origin of DN T cells in MRL/lpr mice found in mice was prone or not prone to lupus, remains unclear and in dispute. Researchers believed that DN T cells originated from activated CD4+ T cells [25-29] and activated CD8+ T cells [30-33] which downregulate CD4 or CD8 receptor expression on their surface. Our results showed that LCHJ suppressed the activation of CD4+ T and CD8+ T cells in MRL/mice, especially significantly decreased the frequency of activated CD8+ T cell. Our results also suggested that the mechanism of how LCHJ, especially when combined with prednisone, decreased the accumulation of DN T cells in MRL/lpr mice, which may be closely associated with the reduced frequencies of activated CD4+ T and CD8+ T cells.

More evidence indicated that T cells play more important roles in SLE compared to B cells [22, 23]. Autoantibody production in MRL/lpr mice promotes the development of lupus and contributes to renal injury [22, 34, 35]. It was believed that plasma cells, which secrete multiple antibodies or autoantibodies in MRL/lpr mice, were originated from B cells. Besides, CD138+ T cells were identified previously in MRL/lpr mice and in patients who suffer from plasmablastic B-cell neoplasms [20, 21]. In the present study, we observed that the majority of CD138+ plasma cells in MRL/lpr mice were CD138+ T cells which expressed both CD3 and CD138. Further evidence that CD138+ T cell frequency in T cells increases as lupus is developed in MRL/lpr mice but not in mice that are not prone to lupus was also provided [22]. Importantly, researchers also demonstrated that CD138+ T cells promote the progression of lupus in MRL/lpr mice and significantly contribute to the production of anti-dsDNA antibody both in vivo and in vitro [22]. In the present study, we observed that LCHJ significantly prevented the accumulation of plasma cells in MRL/lpr mice. Furthermore, the accumulation of CD138+ T cells was also significantly decreased in LCHJ-treated MRL/lpr mice. This indicated that decreased serum anti-dsDNA levels in MRL/lpr mice treated with LCHJ were associated with its accumulation-preventing

effects for CD138+ T cells in MRL/lpr mice. Moreover, LCHJ also significantly decreased CD138+ T cell frequency after 24 h CpGC stimulation in splenocytes. Previous research has demonstrated that CD138+ T cells mainly originate from CD4+CD138- T cells [22]. Further, we also found that LCHJ significantly decreased CD4+CD138 T cells originated from CD4+CD138- T cells in MRL/mice. This resulted in the reduced accumulation of CD138+ T cells in MRL/lpr mice after LCHJ treatment.

Inflammation induced by immune complexes and other activated molecules results in multiple organ injuries and promotes the development SLE in vivo [36]. Previous studies reported increased levels of multiple cytokines in serum in MRL/lpr mice [37]. Here, LCHJ significantly decreased levels of IFN-tiple cytokines in serum in MRL/ecNumlpr mice. Previous research also reported increased inflammation in MRL/lpr mice due to an increased level of multiple cytokines in the serum [37, 38]. It has been demonstrated that serum IFN-γ levels significantly increased in patients with SLE and MRL/lpr mice [37, 39]. IFN-γ dramatically promotes the proliferation of DN T cells and significantly increases the expression of FasL on the surface of DN T cells in MRL/lpr mice [40, 41]. Besides, DN T cells in MRL/lpr mice are strongly cytotoxic, overexpressing FasL, which results in autoimmune injuries of multiple tissues that express small amounts of Fas receptor [23, 42]. These results demonstrate that IFN-γ is involved in lupus development and tissue injuries in MRL/lpr mice. In our study, LCHJ also significantly decreased IFN-γ expression in CD4+ T cells in MRL/lpr mice after both 5 and 48 h of splenocyte stimulation in vitro. These results indicated that LCHJ decreased Th1 cell frequency among CD4+ T cells and reduced IFN-γ serum levels in MRL/lpr mice, and we believe that it prevented DN T cell accumulation and alleviated renal injury in MRL/lpr mice, which was induced by DN T cells.

LCHJ, as a decoction of traditional medicine, has been used for patients with inactive SLE in the clinic and is usually combined with prednisone to prevent active SLE in patients who are in remission. Importantly, LCHJ treatment was chosen and applied to decrease the dose of prednisone for patients with inactive SLE. In the clinic, the application of LCHJ and prednisone combination showed better therapeutic effects and significantly prevented active SLE in patients who were in remission. In the present study, we also investigated the underlying mechanism of how LCHJ combined with prednisone significantly prevents the development of active SLE in patients in remission. LCHJ combined with prednisone showed significant therapeutic effects on MRL/lpr mice. CpGC stimulation was used in this study to mimic *in vivo* conditions of active SLE, i.e. to induce the secretion of IFN-α to promote SLE development and aggravate tissue injury [43-45]. Compared with LCHJ or prednisone treatment alone, combined treatment more significantly prevented the activation and accumulation of T cells in response to CpGC stimulation, especially activation and accumulation of DN T cells, hence leading to a milder response of T cell stimulation. This phenomenon explained why combined LCHJ and prednisone treatment more significantly prevented active SLE in patients who were in remission.

Conclusion

Our results demonstrated that LCHJ has significant therapeutic effects on MRL/lpr mice. LCHJ reduces frequencies of activated CD4+ and CD8+ T cells, decreases Th1 frequency among CD4+ T cells and IFN-γ levels in serum. These result in LCHJ preventing the accumulation of DN T cells in MRL/lpr mice, which further contributes to alleviating renal injuries and the enlargement of spleen and lymph nodes. LCHJ suppresses inflammation in vivo in MRL/lpr mice via decreasing serum IFN-γ, TNF, and IL-6 levels and reducing Th1 frequency among CD4+ T cells. LCHJ prevents the accumulation of plasma cells, and subsequently decreases the production of multiple antibody subsets in MRL/lpr mice. Importantly, LCHJ decreases the frequency of CD4+CD138+ T cells, which originate from CD4+CD138- T cells and further prevents the accumulation of CD138+ T cells in MRL/lpr mice, which contributes to decreased production of anti-dsDNA antibody in vivo in MRL/lpr mice.

Acknowledgements

This work was funded by Postdoctoral Research Activity foundation of Beijing (ZZ2019-23) and the MiaoPu research foundation of the Beijing Institute of Traditional Chinese Medicine (MP-2020-45). We would like to acknowledge Dr Sabry Hamza for editing this manuscript.

Disclosure of conflict of interest

None.

Address correspondence to: Ping Li, Beijing Hospital of Traditional Chinese Medicine, Capital Medical University, Beijing Institute of Traditional Chinese Medicine, Dongcheng, 23 Art Gallery Back Street, Beijing, China. Tel: +86-13167313738; E-mail: liping@bjzhongyi.com; Ping Wang, Department of Dermatology, Beijing Hospital of Traditional Chinese Medicine, Capital Medical University, 23 Art Gallery Back Street, Beijing 100010, China. E-mail: wangpingwpwp@126.com

References

[1] Kaul A, Gordon C, Crow MK, Touma Z, Urowitz MB, van Vollenhoven R, Ruiz-Irastorza G and Hughes G. Systemic lupus erythematosus. Nat Rev Dis Primers 2016; 2: 16039.

[2] Dörner T and Furie R. Novel paradigms in systemic lupus erythematosus. Lancet 2019; 393: 2344-2358.

[3] Lisnevskaia L, Murphy G and Isenberg D. Systemic lupus erythematosus. Lancet 2014; 384: 1878-1888.

[4] Zharkova O, Celhar T, Cravens PD, Satterthwaite AB, Fairhurst AM and Davis LS. Pathways leading to an immunological disease: systemic lupus erythematosus. Rheumatology (Oxford) 2017; 56 Suppl 1: i55-i66.

[5] Stojan G and Petri M. Epidemiology of systemic lupus erythematosus: an update. Curr Opin Rheumatol 2018; 30: 144-150.

[6] Parikh SV, Almaani S, Brodsky S and Rovin BH. Update on lupus nephritis: core curriculum 2020. Am J Kidney Dis 2020; 76: 265-281.

[7] Gergianaki I, Bortoluzzi A and Bertsias G. Update on the epidemiology, risk factors, and disease outcomes of systemic lupus erythematosus. Best Pract Res Clin Rheumatol 2018; 32: 188-205.

[8] Durcan L, O'Dwyer T and Petri M. Management strategies and future directions for systemic lupus erythematosus in adults. Lancet 2019; 393: 2332-2343.

[9] Vukelic M, Li Y and Kyttaris VC. Novel treatments in lupus. Front Immunol 2018; 9: 2658.

[10] Wilhelmus S, Bajema IM, Bertsias GK, Boumpas DT, Gordon C, Lightstone L, Tesar V and Jayne DR. Lupus nephritis management guidelines compared. Nephrol Dial Transplant 2016; 31: 904-913.

[11] Pinheiro SVB, Dias RF, Fabiano RCG, Araujo SDA and Silva ACSE. Pediatric lupus nephritis. J Bras Nefrol 2018; 41: 252-265.

[12] Mok CC, Yap DY, Navarra SV, Liu Z, Zhao M, Lu L, Takeuchi T, Avihingsanon Y, Yu X, Lapid EA, Lugue-Lizardo LR, Sumethkul V, Shen N, Chen S and Chan TM; Asian Lupus Nephritis Network (ALNN). Overview of lupus nephritis management guidelines and perspective from Asia. Int J Rheum Dis 2013; 16: 625-636.

[13] Dammacco R. Systemic lupus erythematosus and ocular involvement: an overview. Clin Exp Med 2018; 18: 135-149.

[14] Vera G and Tsang-A-Sjoe MWP. Treatment targets in SLE: remission and low disease activity state. Rheumatology (Oxford) 2020; 59 Suppl 5: v19-v28.

[15] Thong B and Olsen NJ. Systemic lupus erythematosus diagnosis and management. Rheumatology (Oxford) 2017; 56 Suppl 1: i3-i13.

[16] Gatto M, Zen M, Iaccarino L and Doria A. New therapeutic strategies in systemic lupus erythematosus management. Nat Rev Rheumatol 2019; 15: 30-48.

[17] Zhang Z, Zheng J, Chen M, Qin H and Zhao B. Systemic lupus erythematosus treated with combined therapy of Chinese Medicine and Western Medicine: a clinical follow-up report of 118 clinical cases. Beijing Med 1979; 1: 44-47.

[18] Zhang Z, An J, Liu C, Tang Z, Yang H, Chen X, Cheng F, Wang P, Han B, Chen Y, Zhang Z and Li Y. Clinical and experimental research on the treatment of systemic lupus erythematosus with combined therapy of Chinese Medicine and Western Medicine. Chinese Journal Trad Med Sci Tech 1996; 3: 11-15.

[19] Zhang Z, An J, Liu C, Tang Z, Yang H, Chen X, Cheng F, Wang P, Han B, Chen Y, Zhang Z and Li Y. Treatment of systemic lupus erythematosus with combined therapy of traditional Chinese and Western Medicine. Trad Chinese Med 1996; 29: 64-65.

[20] Pan Z, Chen M, Zhang Q, Wang E, Yin L, Xu Y, Huang Q, Yuan Y, Zhang X, Zheng G and Yuan J. CD3-positive plasmablastic B-cell neoplasms: a diagnostic pitfall. Mod Pathol 2018; 31: 718-731.

[21] Seagal J, Leider N, Wildbaum G, Karin N and Melamed D. Increased plasma cell frequency and accumulation of abnormal syndecan-1plus T-cells in Igmu-deficient/lpr mice. Int Immunol 2003; 15: 1045-1052.

[22] Liu L, Takeda K and Akkoyunlu M. Disease stage-specific pathogenicity of CD138 (Syndecan 1)-expressing T cells in systemic lupus erythematosus. Front Immunol 2020; 11: 1569.

[23] Alexander JJ, Jacob A, Chang A, Quigg RJ and Jarvis JN. Double negative T cells, a potential biomarker for systemic lupus erythematosus. Precis Clin Med 2020; 3: 34-43.

[24] Brandt D and Hedrich CM. TCRαβ+CD3+CD4-CD8- (double negative) T cells in autoimmunity. Autoimmun Rev 2018; 17: 422-430.

[25] Grishkan IV, Ntranos A, Calabresi PA and Gocke AR. Helper T cells down-regulate CD4 expression upon chronic stimulation giving rise to double-negative T cells. Cell Immunol 2013; 284: 68-74.
[26] Zhang D, Yang W, Degauque N, Tian Y, Mikita A and Zheng XX. New differentiation pathway for double-negative regulatory T cells that regulates the magnitude of immune responses. Blood 2007; 109: 4071-4079.
[27] Ezine S, Lucas B, Vicari A, Dautigny N, Vasseur F and Penit C. A novel CD45RA+CD4+ transient thymic subpopulation in MRL-lpr/lpr mice: its relation to non-proliferating CD4-CD8-CD45RA+ tumor cells. Int Immunol 1993; 5: 89-96.
[28] Sauma D, Mora JR, Fierro A, Morales J, Herzog C, Buckel E, Rosemblatt M and Bono MR. Low-dose prednisone accounts for a transient reduction on CD4+ and CD8+ T cells in renal transplant patients under triple therapy. Transplant Proc 2002; 34: 3183-3184.
[29] Hajkova M, Hermankova B, Javorkova E, Bohacova P, Zajicova A, Holan V and Krulova M. Mesenchymal stem cells attenuate the adverse effects of immunosuppressive drugs on distinct T cell subopulations. Stem Cell Rev Rep 2017; 13: 104-115.
[30] Hedrich CM, Rauen T, Crispin JC, Koga T, Ioannidis C, Zajdel M, Kyttaris VC and Tsokos GC. cAMP-responsive element modulator α (CREMα) trans-represses the transmembrane glycoprotein CD8 and contributes to the generation of CD3+CD4-CD8- T cells in health and disease. J Biol Chem 2013; 288: 31880-31887.
[31] Hedrich CM, Crispín JC, Rauen T, Ioannidis C, Koga T, Rodriguez N, Apostolidis SA, Kyttaris VC and Tsokos GC. cAMP responsive element modulator (CREM) α mediates chromatin remodeling of CD8 during the generation of CD3+CD4-CD8- T cells. J Biol Chem 2014; 289: 2361-2370.
[32] Merino R, Fossati L, Iwamoto MI, Takahashi S, Lemoine R, Ibnou-Zekri N, Pugliatti L, Merino J and Izui S. Effect of long-term anti-CD4 or anti-CD8 treatment on the development of lpr CD4-CD8- double negative T cells and of the autoimmune syndrome in MRL-lpr/lpr mice. J Autoimmunity 1995; 8: 33-45.
[33] Ohteki T, Iwamoto M, Izui S and MacDonald HR. Reduced development of CD48B220+ T cells but normal autoantibody production in lpr/lpr mice lacking major histocompatibility complex class I molecules. Eur J Immunol 1995; 25: 37-41.
[34] Hristova MH and Stoyanova VS. Autoantibodies against complement components in systemic lupus erythematosus - role in the pathogenesis and clinical manifestations. Lupus 2017; 26: 1550-1555.
[35] Wang X and Xia Y. Anti-double stranded DNA antibodies: origin, pathogenicity, and targeted therapies. Front Immunol 2019; 10: 1667.
[36] Sandhu V and Quan M. SLE and serum complement: causative, concomitant or coincidental? Open Rheumatol J 2017; 11: 113-122.
[37] Tshilela KA, Ikeuchi H, Matsumoto T, Kuroiwa T, Sakurai N, Sakairi T, Kaneko Y, Maeshima A, Hiromura K and Nojima Y. Glomerular cytokine expression in murine lupus nephritis. Clin Exp Nephrol 2016; 20: 23-29.
[38] Lian F, Wang Y, Chen J, Xu H, Yang X, Liang L, Zhan Z, Ye Y and Chen M. Activation of farnesoid X receptor attenuates liver injury in systemic lupus erythematosus. Rheumatol Int 2012; 32: 1705-1710.
[39] Tan W, Gu Z, Leng J, Zou X, Chen H, Min F, Zhou W, Zhang L and Li G. Let-7f-5p ameliorates inflammation by targeting NLRP3 in bone marrow-derived mesenchymal stem cells in patients with systemic lupus erythematosus. Biomed Pharmacother 2019; 118: 109313.
[40] Balomenos D, Rumold R and Theofilopoulos AN. Interferon-gamma is required for lupus-like disease and lymphoaccumulation in MRL-lpr mice. J Clin Invest 1998; 101: 364-371.
[41] Juvet SC, Han M, Vanama R, Joe B, Kim EY, Zhao FL, Jeon C, Adeyi O and Zhang L. Autocrine IFNγ controls the regulatory function of lymphoproliferative double negative T cells. PLoS One 2012; 7: e47732.
[42] Benihoud K, Bonardelle D, Bob P and Kiger N. MRL/lpr CD4- CD8- and CD8+ T cells, respectively, mediate Fas-dependent and perforin cytotoxic pathways. Eur J Immunol 1997; 27: 415-420.
[43] Menon M, Blair PA, Isenberg DA and Mauri C. A regulatory feedback between plasmacytoid dendritic cells and regulatory B cells is aberrant in systemic lupus erythematosus. Immunity 2016; 44: 683-697.
[44] AAkiyama C, Tsumiyama K, Uchimura C, Honda E, Miyazaki Y, Sakurai K, Miura Y, Hashiramoto A, Felsher DW and Shiozawa S. Conditional upregulation of IFN-α alone is sufficient to induce systemic lupus erythematosus. J Immunol 2019; 203: 835-843.
[45] Lu Q, Shen N, Li XM and Chen SL. Genomic view of IFN-alpha response in pre-autoimmune NZB/W and MRL/lpr mice. Genes Immun 2007; 8: 590-603.